Nuclear Inst. and Methods in Physics Research, A 1046 (2023) 167687

Contents lists available at ScienceDirect

Nuclear Inst. and Methods in Physics Research, A

journal homepage: www.elsevier.com/locate/nima

Sub-25 ps timing measurements with 10×10 cm^2 PICOSEC Micromegas detectors

M. Lisowska [a,b,*], J. Bortfeldt [c], F. Brunbauer [a], G. Fanourakis [d], K.J. Floethner [a,e], M. Gallinaro [f], F. Garcia [g], I. Giomataris [h], T. Gustavsson [i], F.J. Iguaz [h], D. Janssens [a,j,k], A. Kallitsopoulou [h], M. Kovacic [l], P. Legou [h], J. Liu [m], M. Lupberger [e,n], I. Maniatis [a,o], Y. Meng [m], H. Muller [a,n], E. Oliveri [a], G. Orlandini [a,p], T. Papaevangelou [h], M. Pomorski [q], L. Ropelewski [a], D. Sampsonidis [o,r], L. Scharenberg [a,n], T. Schneider [a], L. Sohl [h], M. van Stenis [a], Y. Tsipolitis [s], S.E. Tzamarias [o,r], A. Utrobicic [a], R. Veenhof [a,t], X. Wang [m], S. White [a,u], Z. Zhang [m], Y. Zhou [m]

[a] European Organisation for Nuclear Research (CERN), CH-1211, Geneve 23, Switzerland
[b] Université Paris-Saclay, F-91191 Gif-sur-Yvette, France
[c] Department for Medical Physics, Ludwig Maximilian University of Munich, Am Coulombwall 1, 85748 Garching, Germany
[d] Institute of Nuclear and Particle Physics, NCSR Demokritos, GR-15341 Agia Paraskevi, Attiki, Greece
[e] Helmholtz-Institut für Strahlen- und Kernphysik, University of Bonn, Nußallee 14–16, 53115 Bonn, Germany
[f] Laboratório de Instrumentacão e Física Experimental de Partículas, Lisbon, Portugal
[g] Helsinki Institute of Physics, University of Helsinki, FI-00014 Helsinki, Finland
[h] IRFU, CEA, Université Paris-Saclay, F-91191 Gif-sur-Yvette, France
[i] LIDYL, CEA, CNRS, Universit Paris-Saclay, F-91191 Gif-sur-Yvette, France
[j] Inter-University Institute for High Energies (IIHE), Belgium
[k] Vrije Universiteit Brussel, Pleinlaan 2, 1050 Brussels, Belgium
[l] Faculty of Electrical Engineering and Computing, University of Zagreb, 10000 Zagreb, Croatia
[m] State Key Laboratory of Particle Detection and Electronics, University of Science and Technology of China, Hefei 230026, China
[n] Physikalisches Institut, University of Bonn, Nußallee 12, 53115 Bonn, Germany
[o] Department of Physics, Aristotle University of Thessaloniki, University Campus, GR-54124, Thessaloniki, Greece
[p] Friedrich-Alexander-Universität Erlangen-Nürnberg, Schloßplatz 4, 91054 Erlangen, Germany
[q] CEA-LIST, Diamond Sensors Laboratory, CEA Saclay, F-91191 Gif-sur-Yvette, France
[r] Center for Interdisciplinary Research and Innovation (CIRI-AUTH), Thessaloniki 57001, Greece
[s] National Technical University of Athens, Athens, Greece
[t] Bursa Uluda University, Görükle Kampusu, 16059 Niufer/Bursa, Turkey
[u] University of Virginia, USA

ARTICLE INFO

Keywords:
Gaseous detectors
Micromegas
Multipad
Timing resolution

ABSTRACT

The PICOSEC Micromegas detector is a precise timing gaseous detector based on a Cherenkov radiator coupled to a semi-transparent photocathode and a Micromegas amplifying structure. First single-pad prototypes demonstrated a time resolution below $\sigma = 25$ ps, however, to make the concept appropriate to physics applications, several developments are required. The objective of this work was to achieve an equivalent time resolution for a 10×10 cm^2 area PICOSEC Micromegas detector. The prototype was designed, produced and tested in the laboratory and successfully operated with a 80 GeV/c muon beam. Preliminary results for this device equipped with a CsI photocathode demonstrated a time resolution below $\sigma = 25$ ps for all measured pads. The time resolution was reduced to be below $\sigma = 18$ ps by decreasing the drift gap to 180 μm and using dedicated RF amplifier cards as new electronics. The excellent timing performance of the single-channel proof of concept was not only transferred to the 100-channel prototype, but even improved, making the PICOSEC Micromegas detector more suitable for large-area experiments in need of detectors with high time resolutions.

1. Introduction

The challenges of future High Energy Physics experiments, including high-pile-up environments expected in the High-Luminosity Large Hadron Collider (HL-LHC), have aroused intense interest in the development of technologies for detectors with high time resolution. A time resolution of tens of picoseconds, stable long-term operation and a large area coverage are key requirements that these devices must fulfil to

* Corresponding author.
E-mail address: marta.lisowska@cern.ch (M. Lisowska).

https://doi.org/10.1016/j.nima.2022.167687
Received 31 August 2022; Received in revised form 17 October 2022; Accepted 19 October 2022
Available online 1 November 2022

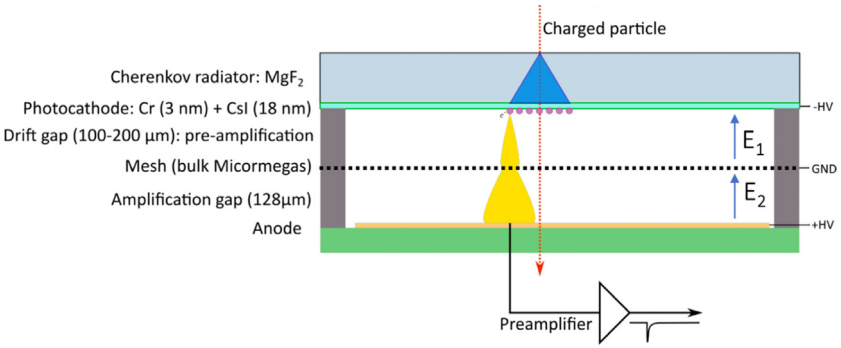

Fig. 1. Schematic representation of the PICOSEC detection concept. A charged particle passing through a Cherenkov radiator creates UV photons that are converted into primary electrons on a photocathode, pre-amplified in the drift gap and multiplied in the amplification gap [2].

be applicable in demanding environments such as the HL-LHC. The first PICOSEC Micromegas (MM) prototype indicated how precise time resolution can be achieved with a single-channel gaseous detector with an active area of 1 cm in diameter [1]. Although the detector's proof of concept demonstrated a $\sigma = 25$ ps time resolution, this excellent timing performance has never been transferred to a 100-channel device. The objective of this work was to achieve an equivalent time resolution for the 100-channel PICOSEC MM detector with an active area of 10×10 cm^2.

In Section 2, the PICOSEC MM detection concept is outlined. Section 3 is a description of the 10×10 cm^2 area PICOSEC MM detector design and production. In Section 4, the electronics dedicated to the 100 channels detector, including custom-made amplifiers and SAMPIC digitiser, are explained. The results from timing measurements obtained for the 10×10 cm^2 multipad detectors are presented and discussed in Section 5. Section 6 gives an outlook of the PICOSEC MM detector robustness aspects that need to be implemented, including resistive MM and robust photocathodes. Section 7 is a summary of the conclusions drawn from this paper.

2. PICOSEC Micromegas detection concept

Within the PICOSEC MM collaboration, a gaseous detector that aims at reaching a time resolution of tens of picoseconds is being developed [1]. The PICOSEC MM detection concept is presented in Fig. 1 . A charged particle passing through a Cherenkov radiator (3 mm thick MgF_2 crystal) creates a cone of UV photons that are converted into photoelectrons on the photocathode. The baseline converter of the UV photons into the photoelectrons for the PICOSEC MM detector is a 18 nm thick Cesium Iodide (CsI) semi-transparent photocathode. Following the extraction of the primary electrons from the photocathode, a high electric field in the drift gap leads to successive ionisations by the primary electrons and thus a pre-amplification. After passing through the MM mesh, the electrons are additionally multiplied in the amplification gap. Both regions are filled with a flammable gas mixture of 80% neon, 10% CF_4 and 10% ethane. The amplified electrons induce a signal on the anode which is passed through an amplifier and readout by a digitiser. A typical PICOSEC MM waveform displaying a fast electron peak and a slow ion tail is presented in Fig. 2. The rising edge of the electron peak is used to calculate the time of arrival.

The first single-pad prototypes demonstrated time resolution below $\sigma = 25$ ps [1]. To make the concept appropriate to physics applications, several developments are required. Since the objective is to build a tileable multi-channel detector modules for large area coverage, the project progressed from a single-pad prototype [1] to a 19-channels device [3] before the current 100-channel module [2] which is the main subject of this study. The active area of the detector changed from 1 cm to 3.6 cm diameter circle between single- and multi-pad prototypes

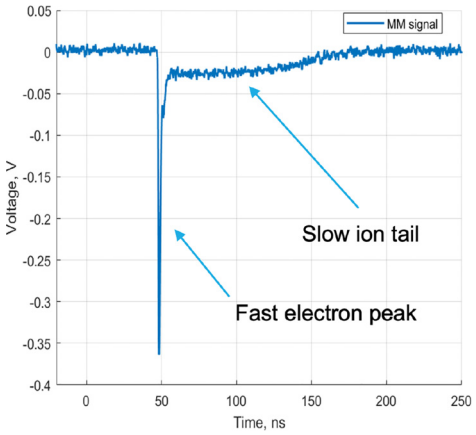

Fig. 2. A typical PICOSEC MM waveform displaying a fast electron peak and a slow ion tail [2].

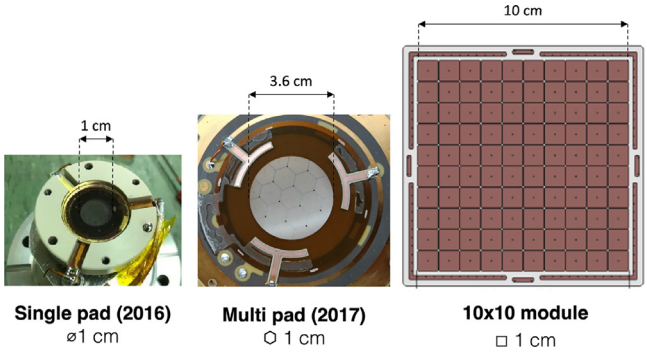

Fig. 3. The evolution of thw PICOSEC MM detectors. From left to right: a single-pad prototype [1], a 19-channels device [3], the 100-channel module [2]. Note that the figures are not in scale.

and it was scaled up to 10×10 cm^2 for the 100-channel module, increasing the surface almost 10 times in comparison to the 19-channels device. The evolution of the PICOSEC MM detectors is presented in Fig. 3. The detector's mechanics, electronics and robustness are some of the developments towards applicable device that are presented in this work.

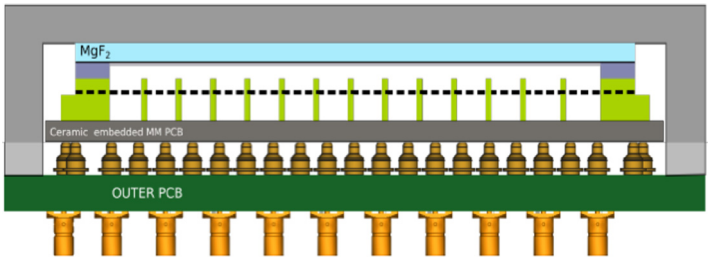

Fig. 4. A new PICOSEC MM detector design consisting of 2 separate PCBs: an outer board screwed to the aluminium housing and a more rigid hybrid ceramic-FR4 MM board. The outer PCB was connected with the MM PCB with spring-loaded pins [2].

3. Design and production of the 10 × 10 cm^2 area PICOSEC Micromegas detector

The PICOSEC MM detectors consist of a printed circuit board (PCB) on top of which a woven mesh of 18 μm thick steel wires is stretched over pillars and a coverlay (Pyralux PC1025) frame. The thickness of the amplification gap is defined by the height of the bottom coverlay and the pillars and chosen to be 128 μm. The thickness of the drift gap is defined by the spacer placed on top of the mesh stretching frame which in the standard configuration is 200 μm.

The first PICOSEC MM multipad prototype was a 19-channels detector with a circular-shaped active area of 3.6 cm in diameter and a PCB made of a 3.2 mm thick FR4 plate [3]. Preliminary measurements of the detector flatness showed deformations in the active area in the range of 30 μm that caused a non-uniform drift gap and resulted in a non-uniform response of the device. The deformations were introduced by mechanical stress on the PCB due to fixing it to the detector flange as well as non-flatness of the PCB because of the forces originating from stretching the mesh on top of it. For scaling-up this prototype, the problem of the deformations was anticipated to be more pronounced for the larger active areas. The requirement for the 10 × 10 cm^2 module was to obtain precise mechanical parts to preserve uniform thickness of the drift gap.

In order to improve the flatness of the active area, the necessary steps were to decouple the PCB from the flange by using a second board called outer PCB and design a more rigid MM PCB [2,4], as can be seen in Fig. 4. To avoid the mechanical connection of the MM PCB to the housing, a new design was made which includes a 6 mm thick outer PCB screwed to the aluminium housing. The outer PCB was connected with the MM PCB with spring-loaded pins. To choose more rigid MM PCB material and its proper thickness, structural simulations of the board deformations under mesh tension were performed using open-source tools: FreeCAD, Gmsh and CalculiX [5]. Based on the experience from the first 19-channels prototype, the main objective for the 10 × 10 cm^2 module was to minimise the deformations below 10 μm throughout the whole active area. The calculations included analysis of how the mesh tension and contact pressure influence the planarity. Simulations suggested that a big gain in planarity can be achieved by a change of the material and only a small increase in the ceramics thickness, as can be seen in Table A.1. The influence of the mesh tension on the planarity of a 4 mm thick ceramic board resulted in maximum calculated displacement in the active area of around 4 μm, which is presented in Fig. 5. The final design of the MM PCB, shown in Fig. 6, consists of a 4.85 mm thick hybrid ceramic-FR4 board instead of a 3 mm thick pure FR4 one.

The production of the hybrid ceramic-FR4 board was monitored with planarity measurements using a Keyence 3D microscope from the beginning of the process [6]. The analysis of the board before the bulking showed that its planarity was within the specifications, as can be seen in Fig. 7. The 100 channels PICOSEC MM detector with flatness deformations below 10 μm was successfully produced, preserving uniform thickness of the drift gap.

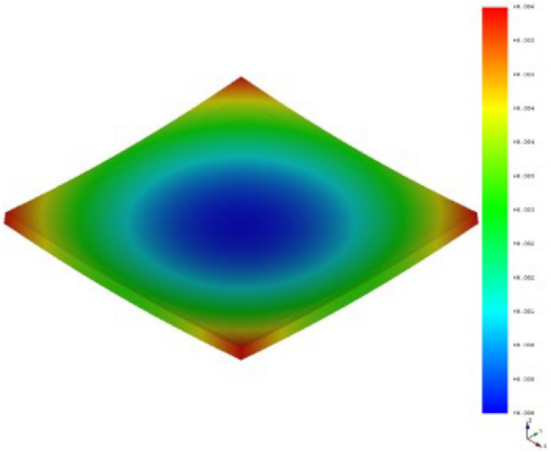

Fig. 5. A simulation of the mesh tension influence on the planarity. For a 4 mm thick ceramic PCB, a maximum displacement in the active area of around 4 μm was calculated [4].

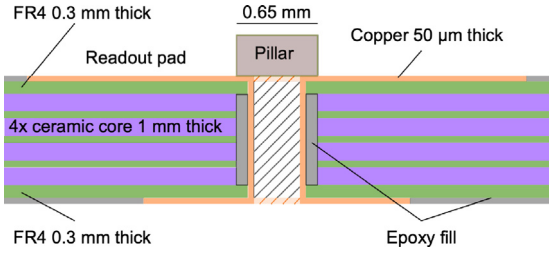

Fig. 6. The final design of the MM PCB consisting of a 4,85 mm thick hybrid ceramic-FR4 board. The anode read-out pads are connected to the back side pads through vias that are plated and filled with conductive epoxy [2].

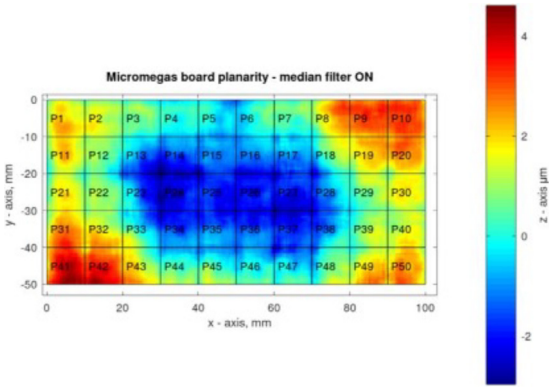

Fig. 7. Planarity measurements of the top half of the PICOSEC Micromegas detector showing flatness deformations below 10 μm [6].

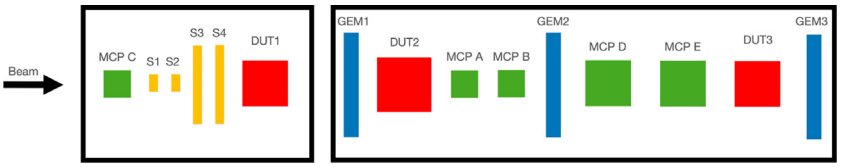

Fig. 8. An example of a telescope configuration consisting of GEM detectors for precise tracking (in blue), MCP-PMTs for timing reference and DAQ (in green) and devices under test (in red). DAQ could also be done by using a coincidence of four scintillators (in yellow).

4. Electronics dedicated to the 100 channels detector

4.1. Custom-made amplifiers

The primary used electronics for amplifying signals induced on the anode was the CIVIDEC C2 [7], a low-noise amplifier with an analog bandwidth of 2 GHz, a gain of 40 dB, and an oscilloscope for digitising waveforms. However, the use of 100 CIVIDECs is highly impractical when it comes to scaling to multiple channels detectors. Therefore, several different types of custom-made amplifiers are being developed. A promising solution are RF pulse amplifier cards optimised for the PICOSEC. The design was based on the RF pulse amplifier for CVD diamond particle detectors [8] and modified with a spark protection up to 350 V, a bandwidth of 650 MHz, a gain of 38 dB and a power consumption of 75 mW per channel [9]. The results obtained for the measurements performed with these amplifiers are presented and discussed in Section 5.4.

4.2. SAMPIC digitiser

After the amplification, the signal needs to be read-out. The baseline digitiser for the PICOSEC MM detector is an oscilloscope with 10 GS/s sampling frequency. Again, the use of 100 oscilloscope channels is highly impractical when it comes to scaling to multiple channels detectors. Therefore, the SAMPIC waveform TDC digitiser [10] is currently being tested. During the last beam campaigns, a 64 channel SAMPIC was tested, while a 128 channel device is being implemented for reading out the PICOSEC MM modules. While the maximum available sampling frequency of currently used SAMPIC modules is limited to 8.5 GS/s, this appears to be sufficient to preserve the timing precision of the PICOSEC MM detectors. The principle of the complete readout chain was proven for the first time by a successful readout of 50 multipad PICOSEC channels.

5. Timing measurements of the 10 × 10 cm^2 area multipad PICOSEC

5.1. Experimental setup

The 100 channels PICOSEC MM detectors were tested in the laboratory and successfully operated during test beam campaigns. The main purpose of the campaigns was to measure timing resolution of the prototypes assembled in different configurations. The measurements were performed at the CERN SPS H4 beam line with a 80 GeV/c muon beam. The main part of the test setup consisted of a beam telescope with triggering, timing and tracking capabilities. An example of a telescope configuration is presented in Fig. 8. The precise tracking of the particles was done using triple-GEMs with a spatial resolution below 80 μm. Multiple micro-channel plate photomultiplier tubes (MCP-PMTs) were used as timing reference and data acquisition (DAQ) trigger. The telescope was built in such a way that it could perform tests of several devices at the same time.

5.2. Time resolution analysis procedure

To properly quantify the timing precision of the PICOSEC detectors, a reference device with better timing precision was required. In the work presented here, an MCP-PMT (R3809U-50 Hamamatsu) with a uniform response in the area of 11 mm in diameter was used as a timing reference of the PICOSEC prototype. The devices were spatially aligned with respect to each other, so when muons passed through them, signals on both detectors were induced. In the analysis, a sigmoid functions were fitted to the leading edges of the electron peaks giving the positions of the signals in time at the 20% Constant Fraction (CF) [2]. The signal arrival time (SAT) was defined as a difference between PICOSEC detector and reference device timing marks. The time resolution of the detector was calculated as a standard deviation of the SAT distribution. The contribution of the MCP-PMT was not subtracted from the time resolution of the PICOSEC detector for all the measurements presented in this work.

5.3. Time response of the multipad PICOSEC in the standard configuration

First test beam measurements of the multipad PICOSEC were performed using the "standard" configuration of the prototype: non-resistive detector with 220 μm drift gap, 3 mm MgF_2 radiator with CsI photocathode and the CIVIDEC amplifier. The aim of the experiment was to obtain timing resolution when signals were fully contained within the centre of individual pads within 5 × 5 mm^2 area. Preliminary results show uniform time resolution of $\sigma = 25$ ps or below for all measured pads [2], confirming that the excellent timing performance can be transferred from a single-pad prototype to a 100-channel module. An example of a SAT distribution of one channel with time resolution, obtained by using the standard deviation, is shown in Fig. 9 and the results from all tested pads are summarised in Table A.2.

When a particle hits the detector in between the pads or in the corner of the active area and the induced signal is not fully contained inside a single channel, the timing capabilities of that channel are reduced [3]. Therefore, sharing of the signal between 4 neighbouring pads was studied in order to test the possibility of timing reconstruction. For this test the same "standard" configuration of the multipad PICOSEC was used. The measurement was performed using the MCP-PMT centred in the cross between 4 channels of the detector and the signals from both devices were sufficiently collected during one run. The experiment confirmed that timing information can be reconstructed when the signal is shared between pads. The obtained time resolution was $\sigma = 30.0$ ps [11,12].

5.4. Time response of the multipad PICOSEC with the custom-made amplifier cards and the reduced drift gap

First test beam measurements with custom-made RF pulse amplifiers optimised for the PICOSEC MM detectors were done as a next step towards the improvement of the time response of the device. Except for the new amplifiers, the detector was in the "standard" configuration. Results from the signals fully contained within the centre of individual pads within 5 × 5 mm^2 area confirmed the improvement of the time

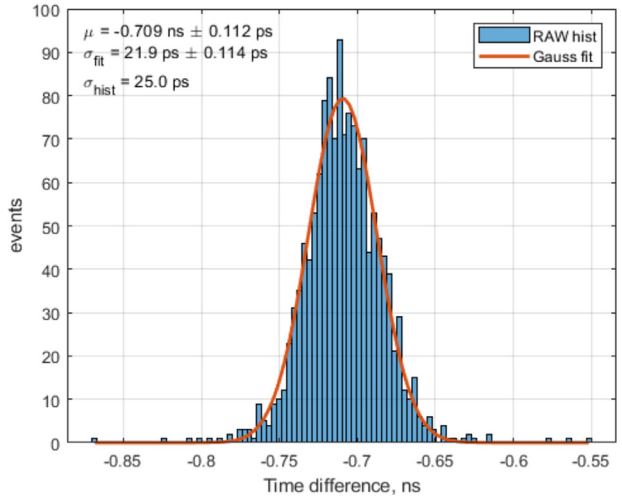

Fig. 9. SAT distribution of one channel of the multipad PICOSEC while performing test beam measurements in the "standard" configuration of the detector. The voltage on the cathode was 500 V and on the anode 275 V. The histogram consist of the data after implementing a geometrical cut which was a 4 mm diameter circle made in the centre of the pad. Time resolution of the measured channel was $\sigma = 25.0$ ps.

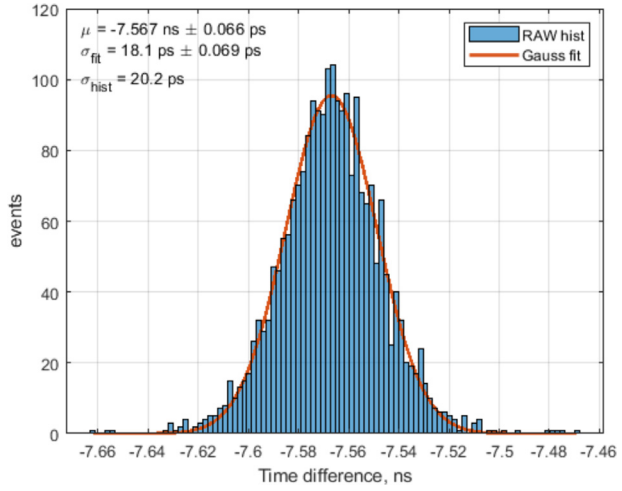

Fig. 10. SAT distribution of one channel of the multipad PICOSEC while performing test beam measurements with the dedicated RF pulse amplifier cards. The voltage on the cathode was 485 V and on the anode 275 V. A geometrical cut of 4 mm diameter circle was made in the centre of the pad. Time resolution of $\sigma = 20.2$ ps was measured.

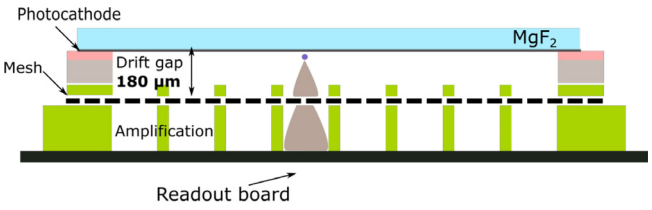

Fig. 11. The PICOSEC MM detector with the drift gap reduced form 220 μm to 180 μm in order to improve time resolution [9].

resolution. This may be attributed to the lower bandwidth, which suppress the noise components, and better impedance matching of the new amplifiers to the detector in comparison to the CIVIDEC electronics. The time resolution obtained for these measurements was below $\sigma =$ 22 ps for all tested pads [9]. An example of a SAT distribution of one channel is shown in Fig. 10 and results from all measured pads are summarised in Table A.3.

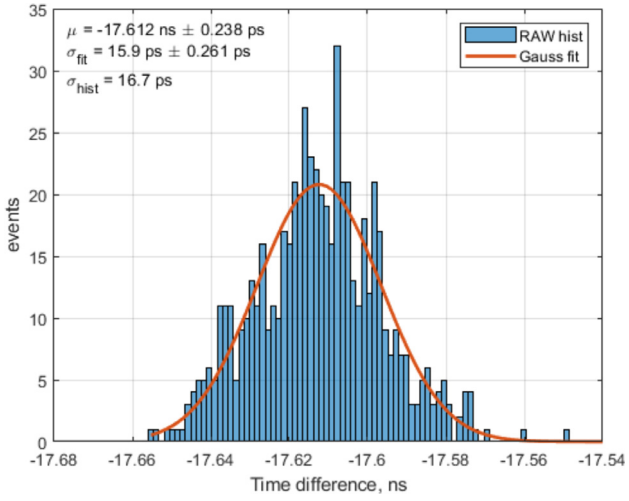

Fig. 12. SAT distribution of one channel of the multipad PICOSEC while performing test beam measurements with the drift gap reduced form 220 μm to 180 μm. A geometrical cut of 4 mm diameter circle was made in the centre of the pad. The voltage on the cathode was 460 V and on the anode 275 V. Time resolution of $\sigma = 16.7$ ps was measured.

A final adjustment towards improving the time resolution of the PICOSEC MM detector was the reduction of the drift gap. The time resolution depends on the SAT which can be reduced by employing a higher drift field [13]. The higher drift field can be achieved by applying higher voltages on the electrodes, however, when too much charge is produced, the operation of the detector becomes unstable. An alternative solution is reducing the thickness of the drift gap. The thinner the gap, the shorter the distance between successive ionisations. For a detector with fixed operating voltages and a decreased drift gap, the electric field is higher, thereby improving the time resolution. At the same time, the distance of the pre-amplification is shorter and the gain is smaller, ensuring a stable operation of the device at a high electric field. Fig. 11 presents a schematic design of the multipad PICOSEC with the drift gap reduced to 180 μm. The measurements of this prototype equipped with a CsI photocathode and the dedicated RF pulse amplifier cards showed a time resolution below $\sigma = 18$ ps for all measured pads [9]. An example of SAT distribution of one channel with time resolution of $\sigma = 16.7$ ps is presented in Fig. 12.

6. Robustness of the PICOSEC Micromegas detector

6.1. Resistive Micromegas

In order to build an applicable device that can be operated in high-rate environments, the PICOSEC MM detector needs to be made more robust. The "standard" configuration of the PICOSEC prototype uses a non-resistive MM detector. Studies on resistive MM are being performed to limit the destructive effect of discharges and achieve stable operation in intense pion beams with a resistive anode. First tests with small area (1 cm in diameter) resistive MM with anode surface resistivities of 292 kΩ/□ and CsI photocathode showed a time resolution of $\sigma = 24.1$ ps. Measurements with small area resistive MM of 82 MΩ/□ and Diamond Like Carbon (DLC) photocathode presented time resolution below $\sigma = 40$ ps, driven by the lower number of photoelectrons produced in the photocathode material. A multipad PICOSEC with 10×10 cm^2 resistive MM of 20 MΩ/□ is being prepared to be measured in the next test beam campaign.

6.2. Robust photocathodes

The first single-pad prototype used a CsI photocathode as a converter of UV photons from the Cherenkov cone into photoelectrons. CsI is characterised by its high quantum efficiency (around 10 photoelectrons produced per minimum ionising particle with 3 mm thick MgF_2 radiator [1]) in comparison to other materials studied up to now. However, it can be easily damaged by ion back flow, sparks, discharges and it is sensitive to humidity. Therefore, there is a need to search for alternative photocathode materials that would be more robust. The most promising candidates are DLC, Boron Carbide (B_4C) or nanodiamonds. First measurements with the multipad PICOSEC with a DLC photocathode, a 220 μm drift gap and CIVIDEC amplifier, showed time resolution of $\sigma = 45$ ps for all measured pads [14]. Additionally, comparative measurements with different thicknesses of B_4C photocathodes in small single-channel prototypes are ongoing.

7. Conclusions

Preliminary results for the 10 × 10 cm^2 area PICOSEC detector demonstrated a time resolution below $\sigma = 25$ ps per pad, showing that the excellent timing performance of the PICOSEC detector's single-channel proof of concept can be transferred to the 100-channel prototype. The best time resolution, below $\sigma = 18$ ps, was obtained for the detector with the 180 μm drift gap, a CsI photocathode and the dedicated RF pulse amplifier cards. The results made the concept more suitable for large-area experiments in need of detectors with high time resolution. Developments towards applicable detectors are ongoing. They include the improvement of stability of the detector by using the multipad PICOSEC with a resistive MM and robustness studies of alternative photocathode materials, e.g. DLC and B_4C. As a next step, a complete readout of a 100 channel prototype with the dedicated RF pulse amplifier cards and SAMPIC waveform TDC digitiser is planned. Additionally, sealed detectors, which are clean, hermetically closed devices with high gas quality, are being developed. Scaling the PICOSEC MM detector to larger area by tiling 10 × 10 cm^2 modules or the development of 20 × 20 cm^2 prototype is considered to be a next step towards applicable devices.

Declaration of competing interest

The authors declare that they have no known competing financial interests or personal relationships that could have appeared to influence the work reported in this paper.

Acknowledgements

We acknowledge the financial support of the EP R&D, CERN Strategic Programme on Technologies for Future Experiments; the RD51 collaboration, in the framework of RD51 common projects; the Cross-Disciplinary Program on Instrumentation and Detection of CEA, the French Alternative Energies and Atomic Energy Commission; the PHENIICS Doctoral School Program of Université Paris-Saclay, France; the Fundamental Research Funds for the Central Universities of China; the Program of National Natural Science Foundation of China (grant number 11935014); the COFUND-FP-CERN-2014 program (grant number 665779); the Fundação para a Ciência e a Tecnologia (FCT), Portugal (grants IF/00410/2012 and CERN/FIS-PAR/0006/2017); the Enhanced Eurotalents program (PCOFUND-GA-2013-60 0382); the US CMS program under DOE contract No. DE-AC02-07CH 11359.

Appendix

See Tables A.1–A.3.

Table A.1
A comparison of the maximum estimated displacement in the active area for PCBs made of different materials and thicknesses given by simulations [4].

PCB material	Thickness [mm]	Displacement [μm]
FR4	3	91
	6	20
	9	10
Hybrid ceramic-FR4	2	17
	3	8
	4	4

Table A.2
Time resolution of all measured pads for the multipad PICOSEC in the "standard" configuration [2].

Pad number	Time resolution [ps]
03	24.6
06	24.1
12	25.0
13	23.9
15	22.1
16	22.9
17	24.7
18	23.0
20	23.0
26	23.9
36	23.9
41	24.0

Table A.3
Time resolution of all measured pads for the multipad PICOSEC with the custom-made amplifier cards [9].

Pad number	Time resolution [ps]
12	21.1
13	19.2
15	20.2
18	19.5
22	18.9
25	20.6
26	20.8
31	21.1
36	21.0
40	20.4

References

[1] F.J. Iguaz, et al., for the PICOSEC Micromegas Collaboration, PICOSEC: Charged particle timing at sub-25 picosecond precision with a Micromegas based detector, Nucl. Instrum. Methods A 903 (2018) 317–325.
[2] A. Utrobicic, for the PICOSEC Micromegas Collaboration, Precise timing measurements with a 10x10 cm2 tileable PICOSEC Micromegas detector module, in: 16th Vienna Conference on Instrumentation, 25th 2022.
[3] S.E. Tzamarias, et al., for the PICOSEC Micromegas Collaboration, Timing performance of a multi-pad PICOSEC-Micromegas detector prototype, Nucl. Instrum. Methods A 993 (2021) 165076.
[4] A. Utrobicic, for the PICOSEC Micromegas Collaboration, Mechanical aspects of CERN GDD 10 cm x 10 cm new PICOSEC detector, in: RD51 Collaboration Meeting, 26th 2020, 2022, Available at https://indico.cern.ch/event/911950/contributions/3912064/. (Accessed 17 October 2022).
[5] FreeCAD open-source tools, 2022, Available at https://www.freecadweb.org. (Accessed 17 October 2022).
[6] A. Utrobicic, for the PICOSEC Micromegas Collaboration, Assembly and gain uniformity measurements of a new large area PICOSEC detector, in: RD51 Collaboration Meeting, 16th 2021, 2022, Available at https://indico.cern.ch/event/989298/contributions/4225012/. (Accessed 17 October 2022).
[7] CIVIDEC instrumentation, broadband diamond amplifier, 2022, Available at https://cividec.at. (Accessed 17 October 2022).
[8] C. Hoarau, et al., RF pulse amplifier for CVD-diamond particle detectors, J. Instrum. 16 (2021) T04005.
[9] A. Utrobicic, for the PICOSEC Micromegas Collaboration, Advancements in a large area 100 channel PICOSEC Micromegas detector module, in: RD51

Collaboration Meeting, 14th 2022, Available at https://indico.cern.ch/event/1138814/contributions/4915978. (Accessed 17 October 2022).

[10] M. Saimpert, et al., Measurements of timing resolution of ultra-fast silicon detectors with the SAMPIC waveform digitizer, Nucl. Instrum. Methods A 835 (2016) 51–60.

[11] A. Kallitsopoulou, for the PICOSEC Micromegas Collaboration, First results in signal sharing with multi-pad picosec module prototypes, in: RD51 Collaboration Meeting, 16th 2021, Available at https://indico.cern.ch/event/1071632/contributions/4607166/. (Accessed 17 October 2022).

[12] I. Maniatis, Research and Development of Micromegas Detectors for New Physics Searches (Ph.D. dissertation), 2022, Available at http://ikee.lib.auth.gr/record/339482/files/GRI-2022-35238.pdf. (Accessed 17 October 2022).

[13] S.E. Tzamarias, et al., for the PICOSEC Micromegas Collaboration, Modeling the timing characteristics of the PICOSEC Micromegas detector, Nucl. Instrum. Methods A 993 (2021) 165049.

[14] A. Utrobicic, for the PICOSEC Micromegas Collaboration, PICOSEC Micromegas detector advancements: multi-pad detector modules, photocathodes and detector studies, in: RD51 Collaboration Meeting, 16th 2021, Available at https://indico.cern.ch/event/1071632/contributions/4612229/. (Accessed 17 October 2022).